

Title	An analysis of volcanic explosions on the basis of the shock-tube model (Nonlinear Wave Phenomena and Applications)
Author(s)	Koyaguchi, Takehiro; Mitani, Noriko K.
Citation	数理解析研究所講究録 (2004), 1368: 9-16
Issue Date	2004-04
URL	http://hdl.handle.net/2433/25401
Right	
Type	Departmental Bulletin Paper
Textversion	publisher

An analysis of volcanic explosions on the basis of the shock-tube model

東京大学・地震研 小屋口剛博, 三谷典子
(Takehiro Koyaguchi¹, Noriko K. Mitani)
ERI University of Tokyo

Abstract

Fluid dynamics of instantaneous volcanic explosions is analyzed as a 1-D shock-tube problem for viscous bubbly magma. When the viscosity of fluid is taken into account, the basic equation of the shock-tube problem is no longer self-similar. The dynamics of viscous bubbly magma after a rapid decompression is explained by a combination of a traveling-wave type solution in the viscous bubbly flow region and a self-similar solution in the inviscid gas-pyroclast flow region.

1 Introduction

The fluid dynamical situation of instantaneous volcanic explosions such as “Vulcanian explosions” is well approximated by a 1-D shock-tube problem (e.g., Turcotte et al., 1990). In Vulcanian explosions, a pressurized bubbly magma (typically 10^1 to 10^2 MPa) is initially separated from the low-pressure air (10^{-1} MPa) by a rock crust. Immediately after the crust is removed, a shock wave propagates into the air and a rarefaction wave propagates into the bubbly magma. The flow of the air and magma is divided into five regions (Fig. 1). Regions 1 and 5 are stationary regions of the air and magma under the initial condition, respectively. Region 2 is a uniform region where the air is compressed after the propagation of the shock wave. Region 3 is another uniform region where magma is decompressed after the propagation of the rarefaction wave. In Region 4 the pressure of magma decreases from Region 5 to 3; this region is called expansion fan. The bubbly magma fragments due to rapid decompression and becomes a dispersion of “pyroclasts” (fine fragments or drops of magma) in the continuous gas phase within Region 4. The gas-pyroclast mixture ejects at a high speed from the volcanic vent, which accounts for explosive features of Vulcanian eruptions.

The transition from the bubbly magma to the gas-pyroclast mixture (i.e., magma fragmentation) is one of the key processes that govern the fluid dynamics of this phenomenon. Before fragmentation, the bubbly magma behaves as a highly viscous flow. On the other hand, after fragmentation, the viscosity of the gas-pyroclast mixture is negligible. We define the boundary between the bubbly magma and gas-pyroclast mixture as fragmentation surface (see Fig. 1). In this note we are particularly concerned with the effects of magma viscosity on the propagation of the fragmentation surface.

¹E-mail: tak@eri.u-tokyo.ac.jp

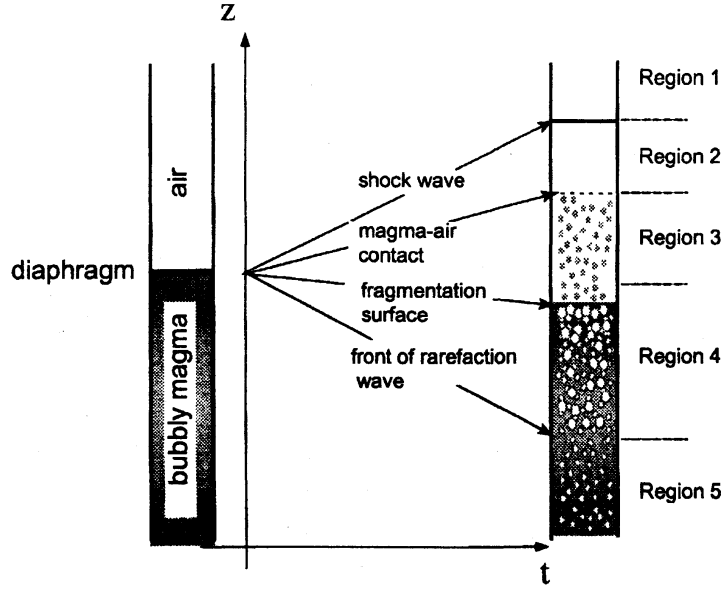


Figure 1: Schematic illustration of “shock-tube problem”. After the diaphragm is removed, five regions can be defined in the air and the bubbly magma. For explanations on individual regions see text.

2 Basic equation

The basic equations for the 1-D flow of magma and air in a cylindrical conduit are given as

$$\frac{\partial \rho}{\partial t} + \frac{\rho w}{\partial z} = 0 \quad : \text{mass conservation} \quad (1)$$

$$\frac{\partial(\rho w)}{\partial t} + \frac{\partial(\rho w^2 + p)}{\partial z} = -\rho g - \rho F_{fric} \quad : \text{momentum conservation} \quad (2)$$

where t , z , w , ρ , p , g are the time, the vertical coordinate, the fluid velocity, the density, the pressure, and the acceleration due to gravity, respectively.

The term of F_{fric} represents the frictional force per unit mass due to shear viscosity and/or wall roughness, and it is commonly expressed as

$$F_{fric} = \begin{cases} \frac{8\eta w}{\rho r^2} & : \text{bubbly magma flow} \\ \frac{f w^2}{4r} & : \text{gas-particle magma flow} \\ 0 & : \text{air flow} \end{cases} \quad (3)$$

where η is the magma shear viscosity and f is a coefficient which is related to roughness of conduit wall and its value is typically 0.01 (cf. Wilson and Head, 1980); in this study f is set to be 0 for simplicity. It is assumed that the flow changes from bubbly flow to gas-pyroclast flow when gas volume fraction exceeds a threshold. Namely,

$$\phi > \phi_{crit}. \quad (4)$$

The equation of the state for the magma-gas mixture can be expressed as

$$\frac{1}{\rho} = \frac{1-n}{\rho_l} + \frac{nRT}{p_g}, \quad (5)$$

where ρ_l is the liquid density, n is the gas mass fraction, R is the gas constant, and T is the temperature. In this study, because the temperature change is negligible due to a large heat capacity of liquid magma, the isothermal condition is assumed.

3 Analyses

Viscosity of magma plays a role in the dynamics of magma flow through F_{fric} in Eq. (2). In order to extract the viscous effect, we carried out supplementary calculations using “inviscid model”, where the effects of viscosity and gravity are neglected by setting $F_{fric} = 0$ and $g = 0$ in Eq. (2). For the inviscid model analytical solutions have already been reported (e.g., Turcotte et al., 1990), which will be reviewed below.

3.1 Inviscid model

The analytical solution for the inviscid case is obtained using the fact that the basic equations (Eqs. (1) and (2)) have a self-similar solution under the boundary condition of the shock-tube problem when $F_{fric} = 0$ and $g = 0$ as

$$\left(\frac{\partial}{\partial t} + (w \pm a) \frac{\partial}{\partial z} \right) (w \pm c) = 0 \quad (6)$$

where

$$c(p) = \int_{\rho_s}^{\rho} \frac{a}{\rho} d\rho = \int_{p_s}^p \frac{dp}{a\rho} \quad (7)$$

and $a(\equiv \sqrt{dp/d\rho})$ is the sound velocity which is given by

$$a = \frac{p}{\rho} \sqrt{\frac{\gamma_m}{nRT}} \quad (8)$$

for the gas-liquid mixture. The subscript s denotes the values of a certain standard state. Here, γ_m is the ratio of specific heat at a constant pressure (C_p) and that at a constant volume (C_v), which is defined as

$$\gamma_m \equiv \frac{C_p}{C_v} = 1 + \frac{nR}{C_v} \sim 1. \quad (9)$$

The equation (6) implies that $w + c$ is conserved along lines of $dz/dt = w + a$ and the quantity $w - c$ is conserved along lines of $dz/dt = w - a$. Since no sound wave propagates forwards in the expansion fan, the quantity $w + c$ is constant throughout Region 2 to 5. Accordingly, the fluid velocity in Region 2 to 4, w_{2-4} , is expressed as a function of pressure, p_{2-4} as

$$\begin{aligned} w_{2-4} &= (w_5 + c_5) - c_{2-4} = c_5 - c_{2-4} \\ &= \int_{p_{2-4}}^{p_5} \frac{dp}{a\rho} \\ &\sim -\sqrt{nRT} \ln \frac{p_{2-4}}{p_5}, \end{aligned} \quad (10)$$

where the subscripts denote the numbers of the regions (cf., Turcotte et al., 1990). Note that $w_2 = w_3$ and $p_2 = p_3$ because of continuity.

Propagation of fragmentation surface

Because fragmentation occurs at a given critical volume fraction (see Eq. (4)), the pressure at the fragmentation surface, p_f , is fixed as

$$p_f = \frac{(1 - \phi_{crit})\rho_l n RT}{\phi_{crit}(1 - n)}. \quad (11)$$

On the other hand, Eq. (6) implies that both $w + c$ and $w - c$, and hence p , w and a , are fixed along each line of $dz/dt = w - a$ in the expansion fan. Therefore, the position of $p = p_f$ propagates at a fixed speed as

$$W_f = w_f - a_f = -\sqrt{nRT} \ln \frac{p_f}{p_5} - \frac{p_f}{\sqrt{nRT}} \left(\frac{nRT}{p_f} + \frac{1 - n}{\rho_l} \right), \quad (12)$$

where W_f is the propagation velocity of the fragmentation surface, and w_f and a_f are the fluid velocity and the sound velocity at $p = p_f$, respectively.

Eq. (12) implies that the velocity of fragmentation surface increases (i.e., downward velocity decreases) as the pressure at the fragmentation surface (p_f) decreases and the initial pressure (p_5) increases. The former tendency is simply explained by the feature of characteristic lines of the expansion fan; $w - a$ increases as pressure decreases in the expansion fan. On the other hand, the dependence on p_5 reflects the fact that the fluid gains more kinetic energy at a given pressure as the initial pressure p_5 increases.

3.2 Viscous model

The basic equations in Section 2 are numerically calculated using CIP and C-CUP methods (Yabe and Aoki, 1991; Yabe and Wang, 1991). Details of the numerical procedure will be reported elsewhere. The numerical results of the viscous model for $r = 10$ m indicate that the effects of magma viscosity play a significant role when viscosity of magma is as large as 10^6 Pas; the pressure gradient becomes much steeper in the bubbly magma due to the effect of large wall friction (Fig. 2a and c).

The effect of viscosity on the propagation velocities of shock wave, magma-air contact and fragmentation surface depends on the sign of W_f . When W_f has a positive sign, viscous bubbly magma must flow upwards before fragmentation. The flow is largely suppressed due to high viscosity of magma, and the velocity of fragmentation surface becomes nearly zero (Fig. 2c and d). Because of this viscous effect, the velocities of shock wave and magma-air contact are largely reduced (Fig. 2d). On the other hand, when W_f has a negative sign, the bubbly magma fragments before it expands. A zone with steep pressure gradient forms just below the fragmentation surface due to high-viscosity of magma in this case, too (Fig. 2a). However, the steep pressure-gradient zone propagates downward together with the fragmentation surface at a speed similar to that of inviscid case; the downward velocity of fragmentation surface slightly decreases (Fig. 2b). The velocities of magma-air contact and shock wave are little affected by the viscosity of the bubbly magma in this case (Fig. 2b).

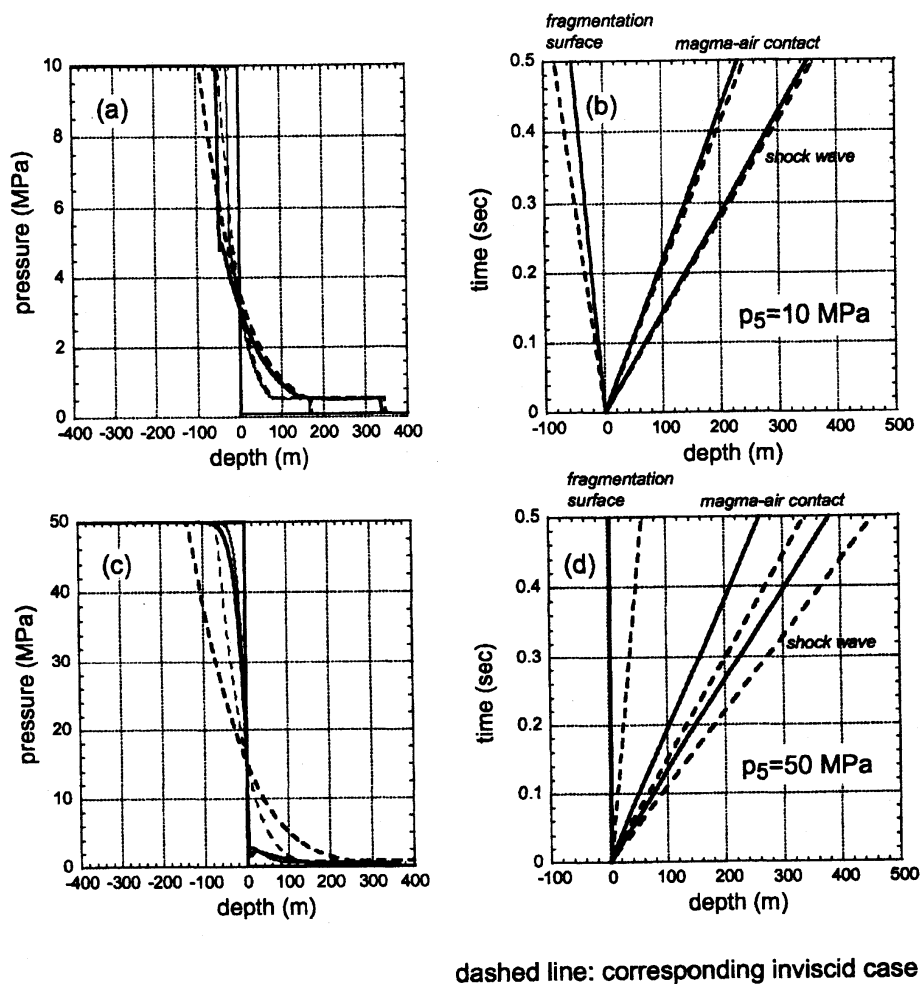


Figure 2: Numerical results of the viscous model ($r = 10$ m and $\eta = 10^6$ Pa s). (a) Pressure profiles at 0.24 sec (thin line) and 0.48 sec (thick line) for $p_5 = 10^7$ Pa, where $w - a$ has a negative value. (b) Positions of shock wave, magma-air contact and fragmentation surface with time for $p_5 = 10^7$ Pa. (c) Pressure profiles at 0.24 sec (thin line) and 0.48 sec (thick line) for $p_5 = 5 \times 10^7$ Pa, where $w - a$ has a positive value. (d) Positions of shock wave, magma-air contact and fragmentation surface with time for $p_5 = 5 \times 10^7$ Pa. The results of the inviscid model are also given by dashed lines.

Traveling-wave type of solution in the bubbly flow region and propagation of fragmentation surface

When the viscous effects play a significant role, $F_{fric} \neq 0$ in Eq. (2) in the bubbly flow region. In such cases, the basic equations are no longer self-similar; the right hand side of Eq. (6) becomes non-zero in the bubbly flow region. Accordingly, the analytical approach for the inviscid case is not applicable. We develop another analytical approach for cases where a fragmentation surface propagates at a constant speed $W_f (< 0)$.

The basic idea of the analytical approach is illustrated in Fig. 3. The numerical results suggest that the pressure profile for the case of $W_f < 0$ is accounted for by the two regions: the viscous bubbly flow region with steep pressure gradient which propagates at the same velocity as the fragmentation surface and the regions of the gas-pyroclast flow and air where pressure profile evolves in the same way as the inviscid case (Fig. 2a). This feature can be explained in the following way. Because the gas-pyroclast flow is approximated to be inviscid, the basic equations in this region can be expressed in the form of Eq. (6)². Therefore, it is expected that there is a self-similar solution in this region which satisfies a boundary condition at the fragmentation surface traveling at W_f as

$$w_f - W_f = a_f = \frac{\sqrt{nRT}}{\phi_f} = \frac{p_f}{\sqrt{nRT}} \left(\frac{nRT}{p_f} + \frac{1-n}{\rho_l} \right), \quad (13)$$

where $\phi_f = \phi_{crit}$. In the bubbly flow region, on the other hand, the decompression wave travels downwards at a constant velocity W_f . Therefore, when $W_f < 0$, there may be a traveling-wave type solution with a constant shape which satisfies Eq. (13) at the fragmentation surface. These solutions in the gas-pyroclast flow region and the bubbly flow region is a solution of the basic equations of the viscous model if they exist. It should be noted, however, that the initial state of this solution is slightly different from the original shock-tube problem; the initial pressure profile is not stepwise, but has the same shape as the traveling-wave type of solution in the bubbly flow region (see Fig. 3). We will attempt to find a traveling-wave type of solution in the bubbly flow region below.

A solution of traveling-wave type is obtained by introducing a new variable $\zeta = W_f t - z$. Using the new parameter, we can rewrite the time and space partial derivatives as

$$\frac{\partial}{\partial t} = W_f \frac{d}{d\zeta} \quad (14)$$

$$\frac{\partial}{\partial z} = -\frac{d}{d\zeta}, \quad (15)$$

respectively. Substituting these relationships into the basic equations, we obtain the equations for mass and momentum conservation as

$$\frac{d\{(W_f - w)\rho\}}{d\zeta} = 0, \quad (16)$$

and

$$(W_f - w) \frac{dw}{d\zeta} = \frac{1}{\rho} \frac{dp}{d\zeta} - \frac{8\eta w}{\rho r^2}, \quad (17)$$

²The effect of gravity is not considered here.

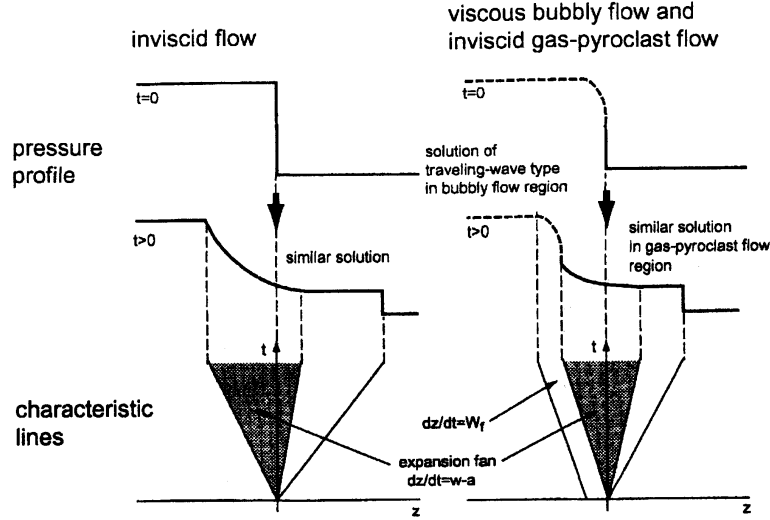


Figure 3: Schematic illustration of the analytical approach of the viscous model.

respectively. After some calculations, Eqs. (16) and (17) is reduced to

$$\frac{dp}{d\zeta} = \frac{8\eta\sqrt{nRT}p_f}{r^2p_5p} \frac{p_5 - p}{1 - \left(\frac{p_f}{p}\right)^2}, \quad (18)$$

which can be integrated to yield

$$-\frac{8\eta\sqrt{nRT}p_f}{r^2p_5} \frac{p_f}{p_5} \zeta = \left(\frac{p_f}{p_5}\right) \left(\frac{p}{p_f} - 1\right) + \left(\frac{p_f}{p_5}\right)^2 \ln \frac{p}{p_f} + \left\{1 - \left(\frac{p_f}{p_5}\right)^2\right\} \ln \frac{p - p_5}{p_f - p_5}, \quad (19)$$

where p_f is given by Eq. (11). Consequently, we obtain the pressure profile of the bubbly region which propagating at W_f (Fig. 4). It is suggested that the normalized pressure profile in the bubbly flow region has a fixed form for a wide range of p_5/p_f . The thickness of the region where the pressure gradient develops is determined by a single parameter as

$$\frac{\zeta^*}{r} = \frac{rp_5}{8\eta\sqrt{nRT}p_f} \frac{p_5}{p_f}. \quad (20)$$

This result is consistent with the numerical result that a region of a steep pressure gradient develops under high-viscosity conditions.

The propagation velocity of the fragmentation surface W_f is obtained from the mass conservation $(w - W_f)\rho = a_f\rho_f = -W_f\rho_5$ as

$$W_f = \frac{\rho_f a_f}{\rho_5} = -\frac{(1 - \phi_{crit})a_f}{1 - \phi_5}. \quad (21)$$

4 Summary

We applied the classical shock-tube model to the problem of instantaneous volcanic explosions. In the problem of volcanic explosions, the effects of magma viscosity are not

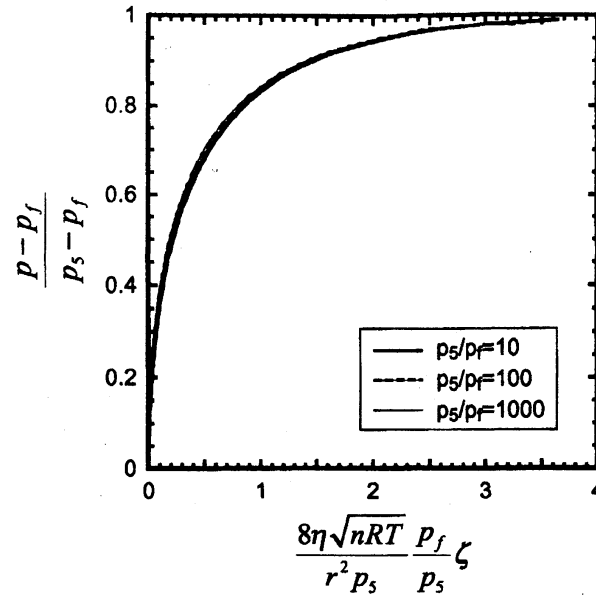


Figure 4: Normalized pressure profile of a traveling type solution of the viscous model for variable p_5/p_f .

negligible in the bubbly flow region. In such cases, the solution is approximated by a combination of a traveling-wave type solution in the bubbly flow region and a self-similar solution in the gas-pyroclast flow region.

References

- [1] Turcotte, D. L., H. Ockendon, J. R. Ockendon and S. J. Cowley (1990) A mathematical model of vulcanian eruptions. *Geophys. J. Int.*, 103, 211-217.
- [2] Wilson, L. and J. W. Head (1981) Ascent and eruption of basaltic magma on the earth and moon. *Jour. Geophys. Res.*, 86, 2971-3001.
- [3] Yabe, T. and T. Aoki (1991) A universal solver for hyperbolic equations by cubic-polynomial interpolation. I. One-dimensional solver. *Comput. Phys. Commun.*, 66, 219-232.
- [4] Yabe, T. and P. -Y. Wang (1991) Unified numerical procedure for compressible and incompressible fluid. *Jour. Phys. Soc. Japan*, 60, 2105-2108.